Angewandte Chemie
Eine Zeitschrift der Gesellschaft Deutscher Chemiker

Supporting Information

Manipulating Reaction Intermediates to Aqueous-Phase ZnSe Magic-Size Clusters and Quantum Dots at Room Temperature

Y. Li, M. Zhang, L. He, N. Rowell, T. Kreouzis, C. Zhang, S. Wang, C. Luan, X. Chen, S. Zhang, K. Yu**

Table of Contents

Experimental Section

Chemicals. Zinc chloride ($ZnCl_2$, 98%) and sodium hydroxide (NaOH, 96%) were obtained from Tianjin Fuchen Chemical. Selenide powder (Se, 99.99%) and sodium borohydride ($NaBH_4$, 98%) were purchased from Alfa-Aesar and Tianjin Damao Chemical, respectively. 3-mercaptopropionic acid (MPA, 99%), butylamine (BTA, 99%), selenourea (SeU, 98%) were purchased from Sigma-Aldrich. Glutathione (GSH, 99%) was obtained from Adamas-beta. All chemicals were used as received without purifications.

Stock solution preparation for $ZnCl_2$ and NaOH. A $ZnCl_2$ stock solution (200.0 mM) was prepared by dissolving $ZnCl_2$ (1.09 g, 8.0 mmol) in deionized water (40.0 mL, including 1% HCl to prevent the hydrolysis of $ZnCl_2$). A NaOH stock solution (about 5.0 M) was obtained by dissolving NaOH (4.00 g, about 100.0 mmol) in deionized water (20.0 mL). By the way, for a SeU solution (80.0 mM) made by dissolving SeU (4.92 mg, 40 µmol) in deionized water (0.5 mL), it was always freshly prepared right before use.

Synthesis of ZnSe PC-299 and QDs with MPA as the ligand. In a typical reaction, $ZnCl_2$ stock solution (200.0 mM, 0.8 mL) and MPA (28 µL, 3.2 mmol) were added in a flask with deionized water (8.2 mL) to result in a colorless and transparent solution. Subsequently, the NaOH stock solution (5.0 M, about 220 µL) was added dropwise until the pH of the aqueous mixture reached 12.0, then a certain volume of water was added to make the total volume to be 9.5 mL. In a side note, white precipitate appeared in the initial stage of the NaOH stock solution addition, which disappeared afterwards with more NaOH addition. It was reported that $Zn(OH)_2$ precipitates at pH 9.0.[1] Subsequently, SeU stock solution (80.0 mM, 0.5 mL) was added under continuously stirring. A transparent and colorless solution was obtained with the feed molar ratio of $4ZnCl_2$/8MPA/2SeU and with the SeU concentration of 4.0 mM. The resulting aqueous mixture was allowed to react at room temperature to produce ZnSe PC-299. After a certain reaction period, an aliquot (100 µL) of the mixture was extracted and dispersed in deionized water (3.0 mL) or a mixture of deionized water (1.5 mL) and BTA (1.5 mL) for absorption measurement.

The approach to ZnSe QDs is similar as that to that for ZnSe PC-299, but with pH 13.0 at room temperature or with pH 12.0 at high temperatures. Furthermore, the synthesis of ZnSe QDs from purified PC-299 was carried out. For the purification of a prenucleation stage sample (from the Figure 1 reaction with the period of 120 min), a large amount of ethanol (~35.0 mL) was added to the reaction (5.0 mL). The resulting turbid solution was then centrifuged at room temperature with a speed of 9500 rpm for about 5 min. After removing the supernatant, the precipitate was oil-like and mixed with ethanol (20.0 mL), and the resulting suspension was centrifuged at 9500 rpm for about 5 min. The procedure was repeated once more, and the precipitate was vacuumed for 4 h at room temperature to remove the solvent residual. The white powder was stored at room temperature, containing mostly PC-299.

Synthesis of ZnSe QDs with GSH as the ligand. The GSH-capped ZnSe QDs was synthesized by using the recipe from the Ref 21 in main text, but with a temperature increase mode from 30 to 90 °C instead of at a constant temperature of 95 °C. Briefly, a sodium hydroselenide (NaHSe) solution (20.0 mM) was prepared first from a mixture of Se powder (32.0 mg, 0.4 mmol) and $NaBH_4$ (38.0 mg, 1.0 mmol) in deionized water (20.0 mL). The obtained NaHSe solution was transparent and colorless, without a trace of undissolved Se powder. A pH 11.5 aqueous solution (40.0 mL) was prepared with NaOH, which contained $ZnCl_2$ (68.0 mg, 0.5 mmol) and GSH (184.0 mg, 0.6 mmol). The freshly prepared NaHSe solution (20.0 mM, 10.0 mL) was added into the aqueous solution (pH 11.5) under vigorous stirring. The resulting mixture had a feed molar ratio of 2.5$ZnCl_2$ to 3GSH to 1NaHSe, with a NaHSe concentration of 4.0 mM. The resulting mixture was slowly heated to 90 °C under a N_2 atmosphere.

Characterizations The absorption spectra were collected between 270 and 600 nm with an interval of 1 nm on a Hitachi UH4150 spectrometer. Deionized water was used as the background. Photoluminescent emission spectra were collected on a F-380 spectrometer, with a 1 nm data collection interval and with an excitation wavelength of 300 nm. For the samples used for the optical measurement, after they were extracted from reactions, an aliquot (100 µL usually, except for Figure 4) of each sample was dispersed in deionized water (3.0 mL) and in a mixture of deionized water (1.5 mL) and BTA (1.5 mL).

^{1}H NMR spectra were collected at 400 MHz on a Bruker Advance II spectrometer. All the ^{1}H NMR spectra collected were corrected by moving the chemical shift of the D_2O solvent peak to 4.70 ppm via the MestReNova software. Matrix-assisted laser desorption/ionization time of flight mass spectrometry (MALDI-TOF MS) spectra were collected on a Shimadzu AXIMA Performance spectrometer with a linear detector and in a positive mode, with 2,5-dihydroxybenzoic acid (DHB) as the matrix. The X-ray photoelectron spectroscopy (XPS) was collected on the AXIS Supra (Kratos). Powder X-ray diffraction (XRD) measurements were performed on an Empyrean X-ray diffractometer (with a Cu Kα radiation) with a θ-θ mode; the data were collected between 10° and 90° with the rate of 10° per minute. Transmission electron microscope (TEM) images were recorded on FEI Tecnai G2 F20 S-TWIN. For the preparation of a TEM grid, one drop of an aqueous sample was placed on the grid, which was then put in a fume hood under ambient conditions for about 12 h to evaporate the solvent.

[1] S. Xu, C. Wang, Q. Xu, H. Zhang, R. Li, H. Shao, W. Lei, Y. Cui, Key Role of Solution pH and Ligands in the Synthesis of Aqueous ZnTe Nanoparticles, *Chem. Mater.* **2010**, *22*, 5838–5844.

Table S1. Literature summary of the aqueous-phase synthesis of ZnSe QDs.

Refs Year	Aqueous-phase reaction	Temperature, period	Absorption peak (nm)
1 2004	5.1Zn(ClO_4)$_2$-12.3MPA-1H_2Se; [Se] = 3.68 mM, pH 6.5	100 °C, 41 h	320–350
2 2006	2ZnCl_2-4.8MPA-1NaHSe; [Se] unknown, pH 6.5	100 °C, 48 h	320–360
3 2007	2.5ZnCl_2-3GSH-1NaHSe; [Se] = 4 mM, pH 11.5	95 °C, 60 min	350–370
4 2007	2Zn(ClO_4)$_2$-4.8MPA-1NaHSe; [Se] unknown, pH 10.5	160 °C, 9 h	Not available
5 2009	2Zn(NO_3)$_2$-2.6MPA-1NaHSe; [Se] = 5 mM, pH 11	100 °C, 50 min	315–360
6 2010	2.5Zn(OAc)$_2$-3GSH-1NaHSe; [Se] = 0.4 mM, pH 11.5	100 °C, 9 h	285–362
7 2013	4Zn(OAc)$_2$-8.5GSH-1$NaSe_2O_3$; [Se] = 0.8 mM, pH 12.2	110 °C, 30 min	~350–375
8 2014	3Zn(NO_3)$_2$-6.6MPA-1NaHSe; [Se] = 1 mM, pH 11.9	90 °C, 6 h	~390
9 2018	2ZnCl_2-2.4CyA-1NaHSe; [Se] unknown, pH 6.0	90 °C, 600 min	327–333
10 2019	2.5Zn(OAc)$_2$-10CECs-1NaHSe; [Se] unknown, pH 8	80 °C	Not available

GSH: glutathione; MPA: 3-mercaptopropionic acid; CyA: cysteamine; CECs: N-(2-carboxyethyl)chitosans. 160 °C is the oil-bath temperature (Ref 4).

[1] A. Shavel, N. Gaponik, A. Eychmüller, Efficient UV-Blue Photoluminescing Thiol-Stabilized Water-Soluble Alloyed ZnSe(S) Nanocrystals, *J. Phys. Chem. B* **2004**, *108*, 5905–5908.

[2] H. Qian, X. Qiu, L. Li, J. Ren, Microwave-Assisted Aqueous Synthesis: A Rapid Approach to Prepare Highly Luminescent ZnSe(S) Alloyed Quantum Dots, *J. Phys. Chem. B* **2006**, *110*, 9034–9040.

[3] Y. Zheng, Z. Yang, J. Y. Ying, Aqueous Synthesis of Glutathione-Capped ZnSe and $Zn_{1-x}Cd_xSe$ Alloyed Quantum Dots, *Adv. Mater.* **2007**, *19*, 1475–1479.

[4] G. Lan, Y. Lin, Y. Huang, H. Chang, Photo-Assisted Synthesis of Highly Fluorescent ZnSe(S) Quantum Dots in Aqueous Solution, *J. Mater. Chem.* **2007**, *17*, 2661–2666.

[5] Z. Deng, F. L. Lie, S. Shen, I. Ghosh, M. Mansuripur, A. J. Muscat, Water-Based Route to Ligand-Selective Synthesis of ZnSe and Cd-Doped ZnSe Quantum Dots with Tunale Ultraviolet A to Blue Photoluminescence, *Langmuir* **2009**, *25*, 434–442.

[6] J. Zhang, J. Li, J. Zhang, R. Xie, W. Yang, Aqueous Synthesis of ZnSe Nanocrystals by Using Glutathione As Ligand: The pH-Mediated Coordination of Zn^{2+} with Glutathione, *J. Phys. Chem. C* **2010**, *114*, 11087–11091.
[7] S. Fu, Q. Sun, D. Li, M. Dong, S. Liu, C. Huang, A Novel One-Pot Synthesis of UV-Blue ZnSe Nanocrystals in Aqueous Solution, *J. Chin. Chem. Soc.* **2013**, *60*, 309–313.
[8] Y. Wang, C. Wang, S. Xu, Z. Wang, Y. Cui, Cation-Inverting-Injection: A Novel Method for Synthesis of Aqueous ZnSe Quantum Dots with Bright Excitionic Emission and Suppressed Trap Emission, *Nanotechnology*, **2014**, *25*, 295602.
[9] I. M. Moura, P. E. C. Filho, M. A. Seabra, G. Pereira, G. A. Pereira, A. Fontes, B. S. Santos, Highly Fluorenscent Positviely Charged ZnSe Quantum Dots for Bioimaging, *J. Lumin*, **2018**, *201*, 284–289.
[10] S. Bratskaya, K. Sergeeva, M. Konovalova, E. Modin, E. Svirshchevskaya, A. Sergeev, A. Mironenko, A. Pestov, Ligand-Assisted Synthesis and Cytotoxicity of ZnSe Quantum Dots Stabilized by N-(2-carboxyethyl)chitosans, *Colloids Surf. B Biointerfaces* **2019**, *182*, 110342.

Table S2. Summary of the reaction variables used in this work.

Figures	Reactions	Se concentrations	pH	Temperatures
1 S1-1, S1-2	$4ZnCl_2$-8MPA-1SeU	4 mM	12	RT
S1-3	0.5/1/2/8$ZnCl_2$-8MPA-1SeU	4 mM	12	RT
S1-4	$4ZnCl_2$-4/16MPA-1SeU	4 mM	12	RT
2 S2-1	$4ZnCl_2$-8MPA-1SeU	1/2/8 mM	12	RT
3	$4ZnCl_2$-8MPA-1SeU	4 mM	13	RT
S3-3	$4ZnCl_2$-8MPA-1SeU	4 mM	9/10/11	RT
4	$4ZnCl_2$-8MPA-1SeU, purified	4 mM	12	25–80 °C
S4-1	$4ZnCl_2$-8MPA-1SeU	4 mM	12	50 °C
S4-2	$4ZnCl_2$-8MPA-1SeU	4 mM	12	30–80 °C
5 S5-1	$2.5ZnCl_2$-3GSH-1NaHSe	4 mM	11.5	30–90 °C

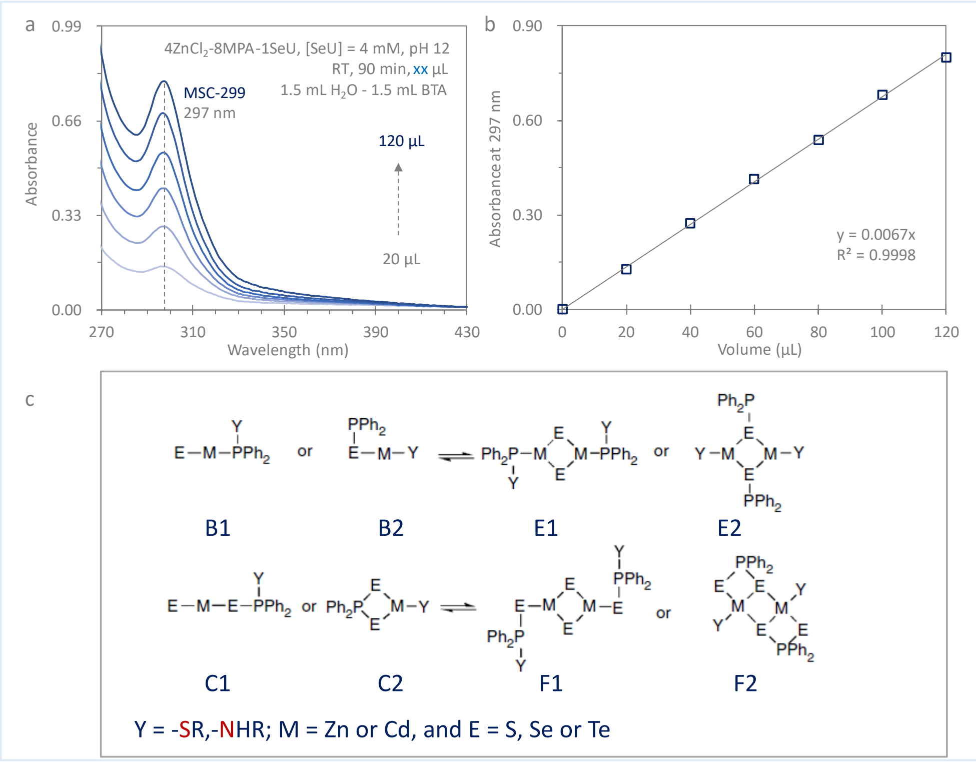

Figure S1-1. Relation between MSC-299 and the ZnSe prenucleation stage sample. A 90 min prenucleation stage sample was prepared from a similar room-temperature reaction for Figure 1. With the amount of 20, 40, 60, 80, 100, and 120 µL, the sample was dispersed in the mixture of H_2O (1.5 mL) and BTA (1.5 mL) for the absorption measurement (a). The absorption strength at 297 nm for MSC-299 (y axis) is plotted as a function of the sample volume (µL) (x axis) (b). A linear relationship between the MSC-299 amount and the sample volume is obtained, y = 0.0067x, R^2 = 0.9998. Thus, the MSC-299 amount can be used to indicate the PC-299 amount in the sample. For the BTA-induced isomerization from PC-299 to MSC-299, Part c provides our explanation based on a previous study that different ligands (Y) favor different isomers.[1] B1 and B2 are a pair of isomers, and C1 and C2 are another pair of isomers. E1 and E2 are the corresponding dimers of B1 and B2, while F1 and F2 are the corresponding dimers of C1 and C2. The isomers have different binding skeletons. They are possible intermediates in reactions towards ME QDs with $EPPh_2H$ as a E precursor. Relatively stable isomers are suggested with different ligands. For CdSe, B2 and C2 and thus E2 and F2 are relatively stable with Y = -SR, while B1 and C1 and thus E1 and F1 are with Y = -NHR.

[1] K. Yu, X. Liu, T. Qi, H. Yang, D. M. Whitfield, Q. Y. Chen, E. J. C. Huisman, C. Hu, General Low-Temperature Reaction Pathways from Precursors to Monomers before Nucleation of Compound Semiconductor Nanocrystals, *Nat. Commun.* **2016**, *7*, 12223.

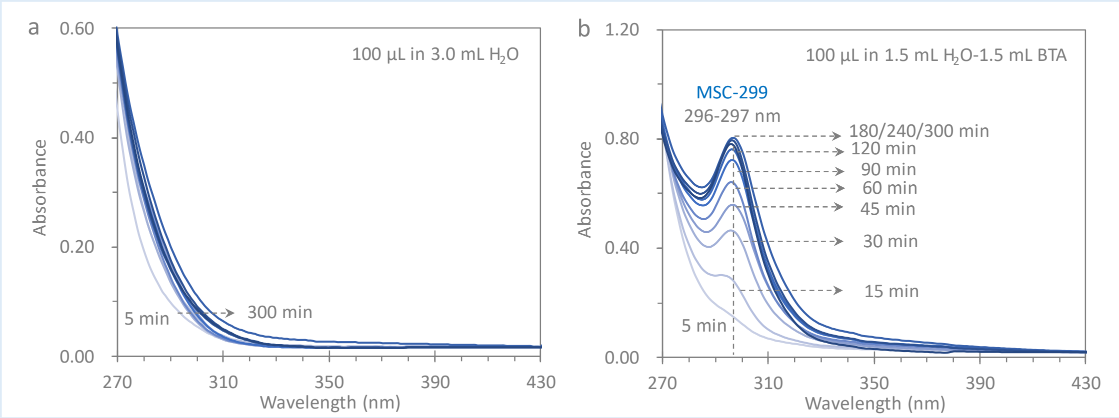

Figure S1-2. The optical absorption spectra of the 10 samples from the Figure 1 reaction. The reaction is $4ZnCl_2$-8MPA-1SeU with a SeU concentration of 4 mM and pH 12 (by a pH meter). An aliquot of 100 µL of each sample was dispersed in 3.0 mL H_2O (a) and in a mixture of 1.5 mL H_2O and 1.5 mL BTA (b). The reaction proceeds in the prenucleation stage and the optically transparent ZnSe PC-299 (a) transforms to absorption ZnSe MSC-299 (b).

Figure S1-3. Optical absorption spectra collected from four room-temperature reactions. With pH 12 and a SeU concentration of 4 mM, the reactions have the feed molar ratio of 0.5/1/2/4$ZnCl_2$-8MPA-2SeU. Samples were taken as indicated from each reaction, and dispersions were prepared with an aliquot (100 µL) of sample in 3.0 mL H_2O (left panel) and in a mixture of 1.5 mL H_2O and 1.5 mL BTA (right panel). It is evident that QDs are produced in the first three reactions (a to f), but not in the last reaction (g and h) that has a high Zn to Se feed molar ratio that favors Step 1 more. It seems difficult to have a simple answer to the question as to which reaction has a larger reactivity. The existence of Step 1 assists us in re-evaluating previous experiment data for a better understanding of the nucleation and growth of colloidal semiconductor QDs.[1-3] "… it is safe to conclude that the number of nanocrystals (nuclei) formed in the initial nucleation stage increased significantly with decreasing initial oleic acid concentration."[1]

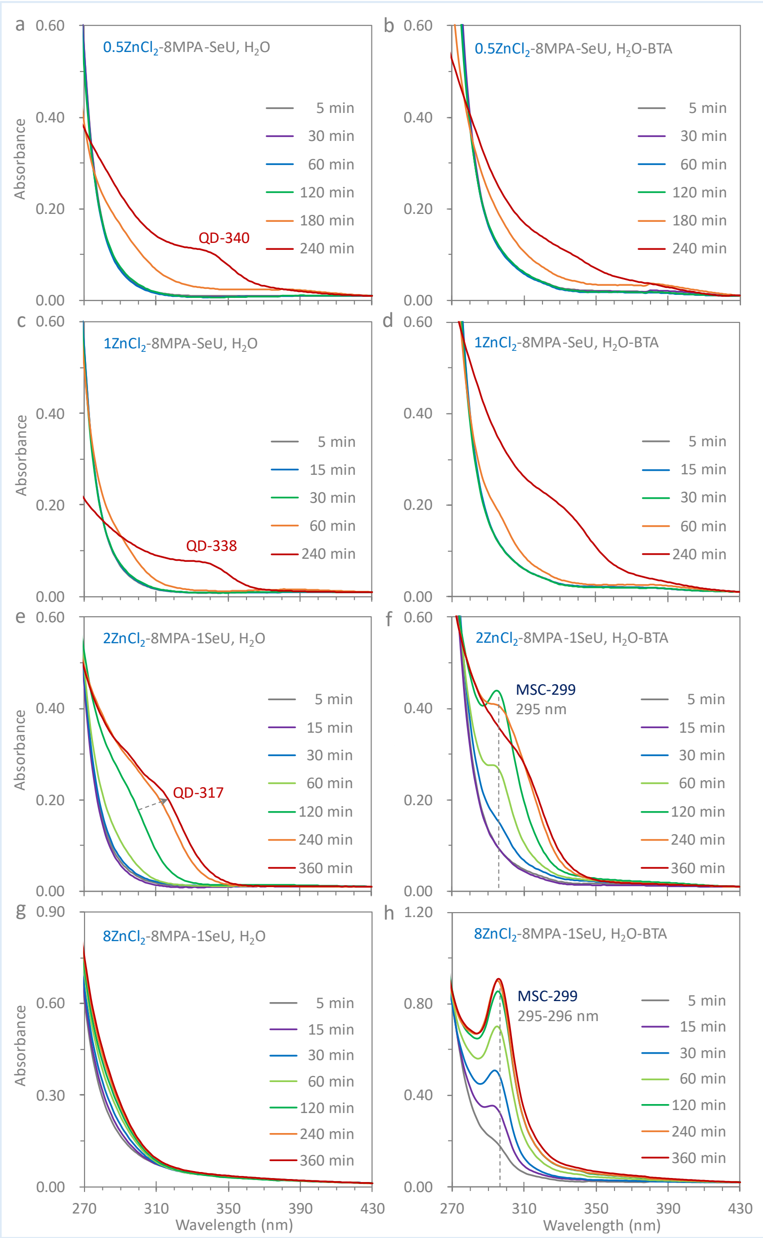

[1] W. W. Yu, X. Peng, Formation of High-Quality CdS and Other II-VI Semiconductor Nanocrystals in Noncoordinating Solvents: Tunable Reactivity of Monomers, *Angew. Chem. Int. Ed.* **2002**, *41*, 2368–2371.

[2] J. Ouyang, J. Kuijper, S. Brot, D. Kingston, X. Wu, D. M. Leek, M. Z. Hu, J. A. Ripmeester, K. Yu, Photoluminescent Colloidal CdS Nanocrystals with High Quality via Noninjection One-Pot Synthesis in 1-Octadecene, *J. Phys. Chem. C* **2009**, *113*, 7579–7593.

[3] S. Bratskaya, K. Sergeeva, M. Konovalova, E. Modin, E. Svirshchevskaya, A. Sergeev, A. Mironenko, A. Pestov, Ligand-Assisted Synthesis and Cytotoxicity of ZnSe Quantum Dots Stabilized by N-(2-carboxyethyl)chitosans, *Colloids Surf. B Biointerfaces* **2019**, *182*, 110342.

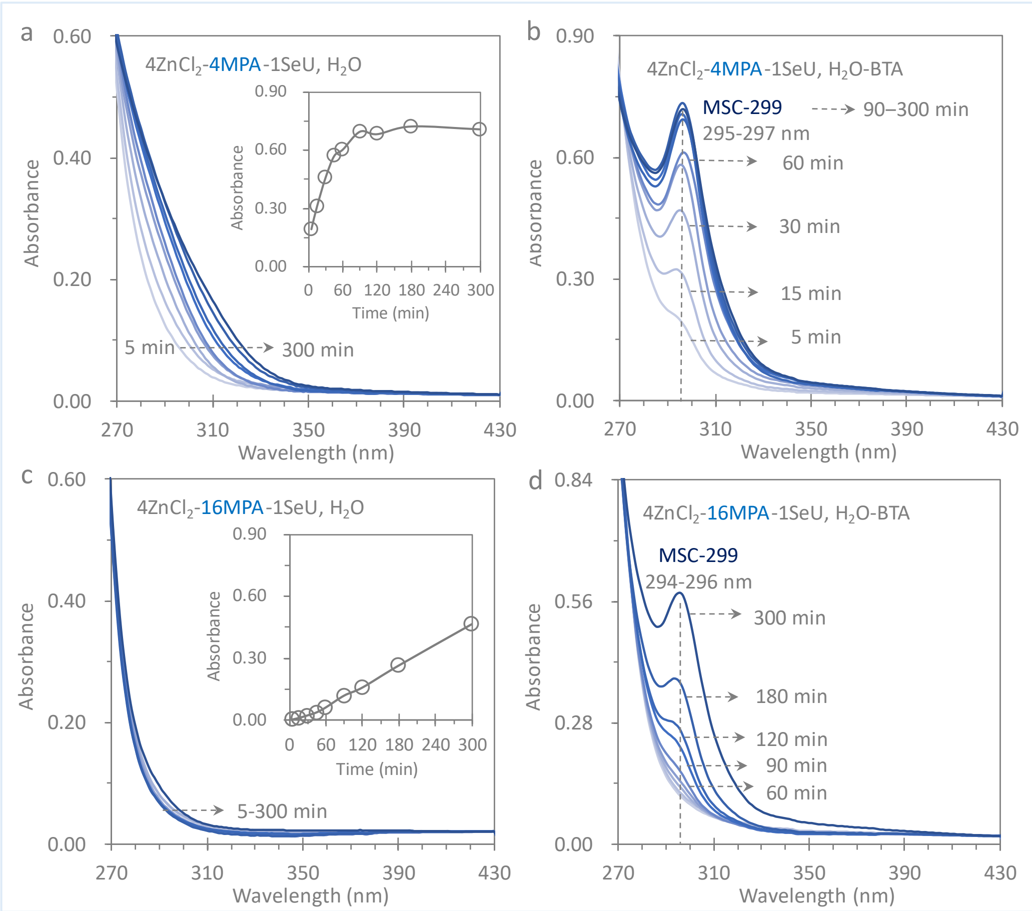

Figure S1-4. Optical absorption spectra collected from two room-temperature reactions. With pH 12 and a SeU concentration of 4 mM, the reactions have the feed molar ratio of $4ZnCl_2$-4MPA-1SeU (top panel a and b) and $4ZnCl_2$-16MPA-1SeU (bottom panel c and d). Nine samples were extracted from reactions within 300 min from each reaction. Dispersions were prepared with an aliquot (100 µL) of sample in 3.0 mL H_2O (left panel a and c) and in a mixture of 1.5 mL H_2O and 1.5 mL BTA (right panel b and d). The insets of a and c summarize the temporal evolution of MSC-299 in b and d, respectively. The presence of a large amount of acid in the latter reaction slows down the formation of Zn and Se covalent bonds. Thus, the formation of PC-299 (Step 1) is retarded, together with that of QDs (Step 3). The previously study on the effect of the acid amount on the nucleation and growth of QDs may be revisit.[1]

[1] J. Ouyang, J. Kuijper, S. Brot, D. Kingston, X. Wu, D. M. Leek, M. Z. Hu, J. A. Ripmeester, K. Yu, Photoluminescent Colloidal CdS Nanocrystals with High Quality via Noninjection One-Pot Synthesis in 1-Octadecene, *J. Phys. Chem. C* **2009**, *113*, 7579–7593.

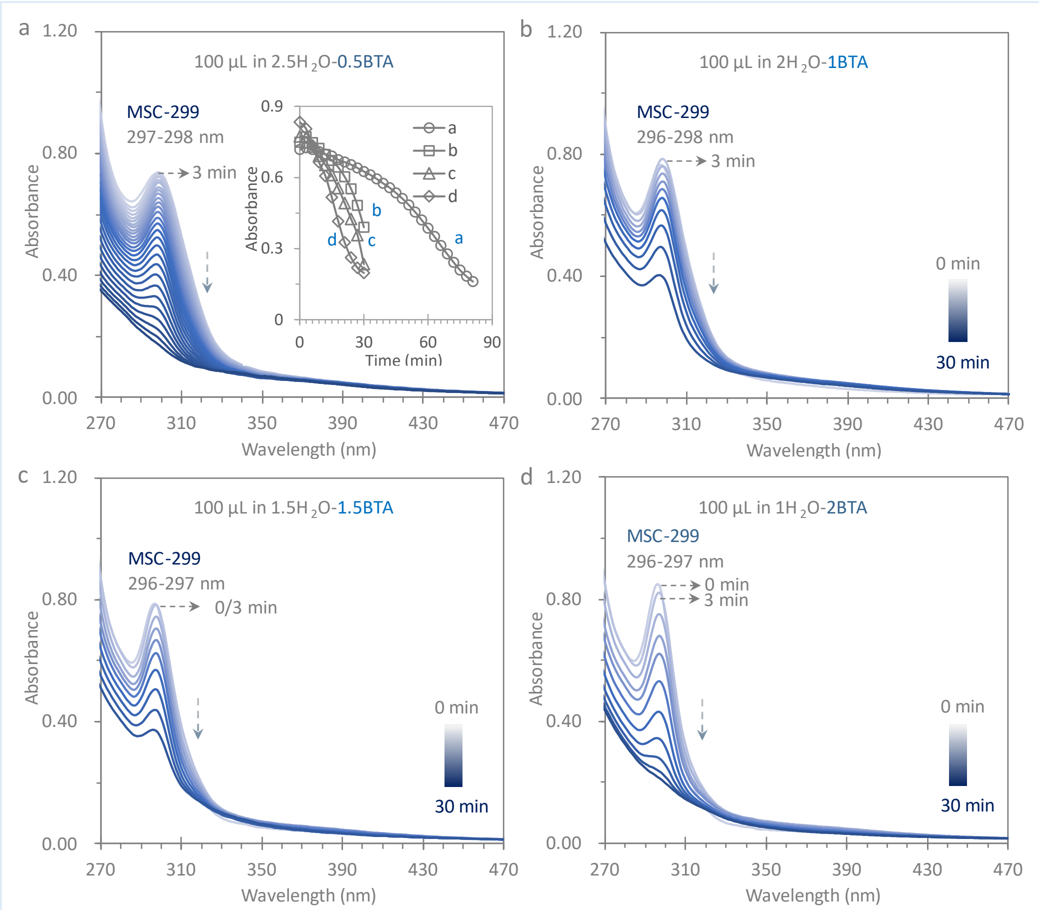

Figure S1-5. Effect of the BTA amount in dispersion on MSC-299 (Step 2). Optical absorption spectra were in situ collected with an interval of 3 min from four dispersions within 80 (a) and 30 min (b to c). A prenucleation stage sample was prepared at room temperature with the reaction period of 120 min from a reaction used for Figure 1. The sample (100 μL) was dispersed in the 3.0 mL mixture of H_2O and BTA, with the BTA amount of 0.5 (a), 1.0 (b), 1.5 (c), and 2.0 mL (d). MSC-299 displays the largest absorption strength in the first 3 min, with the apparent OD of 0.73/3min (a), 0.77/3min (b), 0.77/0min (c), and 0.83/0min (d). The inset in Part a summarizes the temporal evolution of MSC-299 in a to d. Thus, the mixture (c) of H_2O (1.5 mL) and BTA (1.5 mL) is used for the optical absorption measurement.

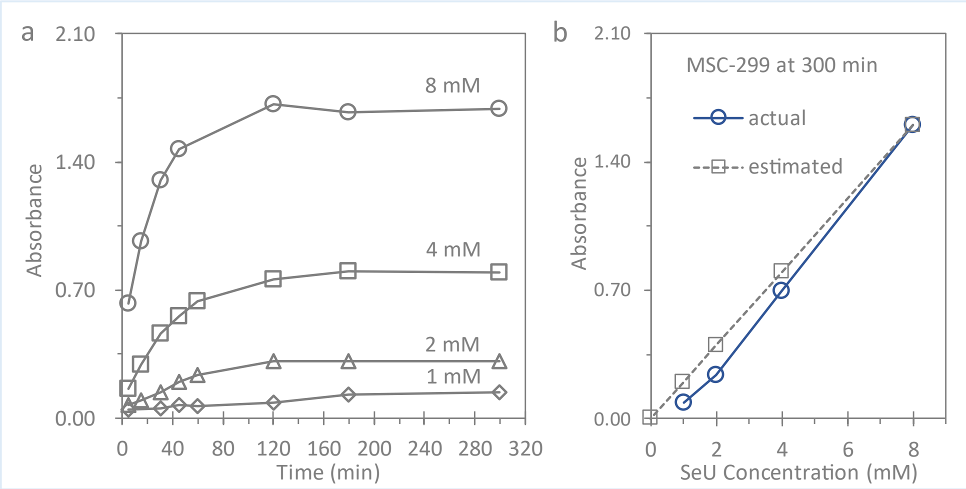

Figure S2-1. Feed concentrations affecting how Step 1 and Step 3 compete. Part a is the temporal evolution of MSC-299 from the four room-temperature reactions of $4ZnCl_2$-8MPA-1SeU with pH 12 and the SeU concentrations of 8 (circles, Figure 2), 4 (squares, Figure S1-2), 2 (triangles, Figure 2), and 1 mM (rhombuses, Figure 2). Part b is for our estimation of the competition between Step 1 and Step 3 in the four reactions. The MSC-299 strength is used to estimate the PC-299 amount produced. With 100% (Step 1) in the 8 mM reaction, the absorption strength of MSC-299 measured (blue circles linked by a solid line) is smaller than the estimated (grey squares linked by a dashed line). The actual values are the 300 min values measured. The estimated values are obtained under the assumption that Step 3 is not active as well for the remaining three batches. We now assess the percentage of molecules that form PC-299 (Step 1, P_1) and Mo/Fr (Step 3, P_2) with Equations 1 and 2:

$$P_1 = \frac{A_{actual}}{A_{estimated}} \times 100\% \qquad (1)$$

$$P_2 = (1 - P_1) \times 100\% \qquad (2)$$

A_{actual} and $A_{estimated}$ are the absorbance values represented by the circular and square symbols, respectively. For the 4 mM batch, it is 0.70/0.80 = 88% (Step 1) and 12% (Step 3). For the 2 mM batch, it is 0.24/0.40 = 60% (Step 1) and 40% (Step 3). For the 1 mM batch, it is 0.09/0.20 = 45% (Step 1) and 55% (Step 3). It is evident that the Step 1 is promoted more at high reaction concentrations.

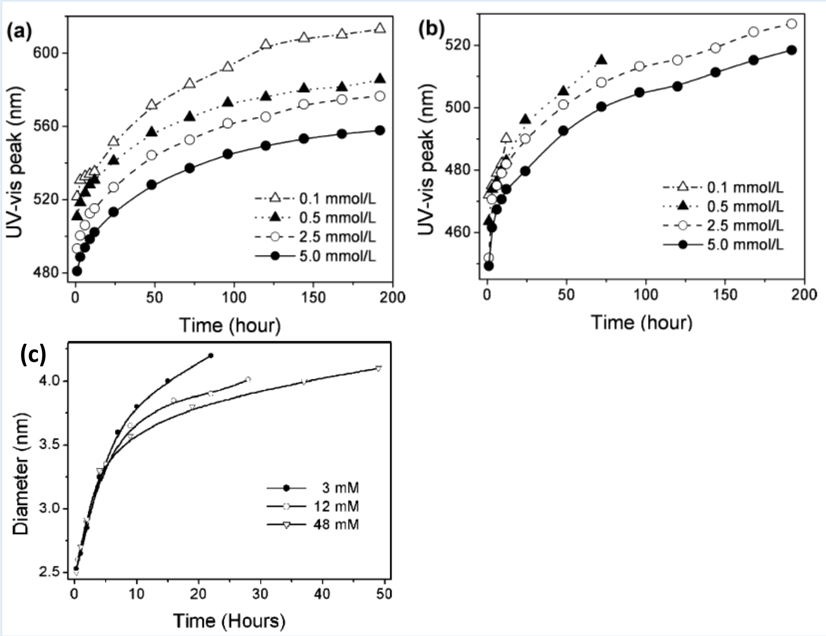

Figure S2-2. Feed concentration effect on the growth of aqueous-phase CdTe QDs.[1,2] Parts a and b are from Ref 1 Figure 5 ($CdCl_2$ + MPA + NaHTe with N_2H_4 for a and NH_3 for b), and Part c from Ref 2 Figure 1 ($CdCl_2$ + MPA + NaHTe). When the feed concentration is relatively low, the size of the resulting QDs is relatively large. The feed concentration effect on the growth of aqueous-phase QDs has been explored in an extremely limited fashion, the present study (Scheme 1) provides a better understood with the consideration of the competition between Step 1 and Step 3. A relatively high feed concentration favors the production of CdS MSCs.[3]

[1] J. Han, X. Luo, D. Zhou, H. Sun, H. Zhang, B. Yang, Growth Kinetics of Aqueous CdTe Nanocrystals in the Presence of Simple Amines, *J. Phys. Chem. C* **2010**, *114*, 6418–6425.

[2] H. Zhang, D. Wang, B. Yang, H. Mohwald, Manipulation of Aqueous Growth of CdTe Nanocrystals to Fabricate Colloidally Stable One-Dimensional Nanostructures, *J. Am. Chem. Soc.* **2006**, *128*, 10171–10180.

[3] D. R. Nevers, C. B. Williamson, B. H. Savitzky, I. Hadar, U. Banin, L. F. Kourkoutis, T. Hanrath, R. D. Robinson, Mesophase Formation Stabilizes High-Purity Magic-Sized Clusters, *J. Am. Chem. Soc.* **2018**, *140*, 3652–3662.

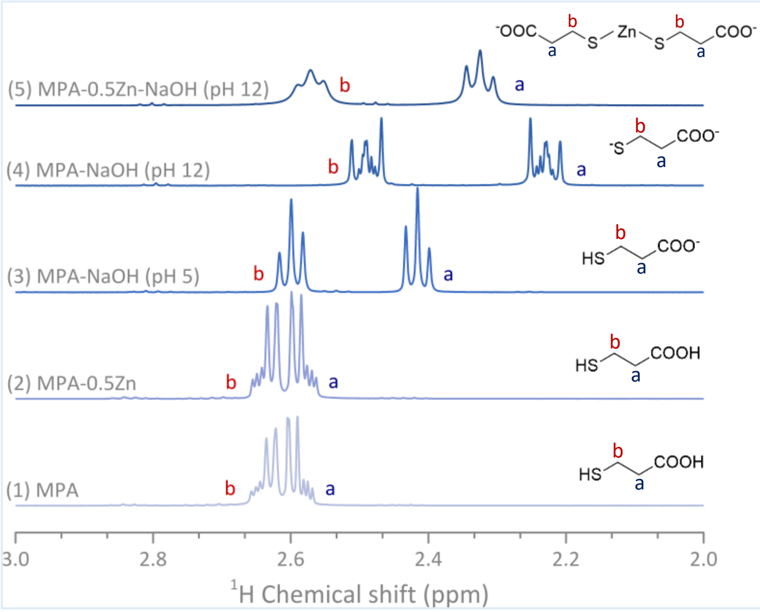

Figure S3-1. ^{1}H NMR study of the formation of Zn-MPA complex. Five MPA-containing solutions in D_2O, as indicated, have a MPA concentration of 20 mM. The feed molar ratio was 1MPA to 0.5Zn (Traces 2 and 5). The two protons of the two methylene groups of MPA are labelled as a and b, which are respectively next to the carboxylic group (-COOH) and the thiol (-SH) group. The NMR study suggests the formation of a Zn-MPA complex (Trace 5). For the characteristic signal of the MPA molecule in D_2O around 2.61 ppm (Trace 1), Trace 2 is quite similar to Trace 1, indicating that there is almost no interaction between $ZnCl_2$ and MPA. For Trace 3 with pH of 5 (estimated by pH test paper and not a pH meter), the spectrum shows two sets of triplet resonance signals, one around 2.60 ppm (Proton b) and the other around 2.41 ppm (Proton a, due to the -COOH deprotonation). For Trace 4 with pH of 12 (by pH test paper), these two sets of triplet signals display upfield shifts to about 2.49 ppm (Proton b, due to the -SH deprotonation) and 2.22 ppm (Proton a), respectively. The pKa value is 4.3 for -COOH and is 10.8 for -SH in MPA.[1-3] Trace 5 displays 2.57 ppm for Proton b and 2.32 ppm for Proton a, due to the formation of Zn-MPA complex, together with relatively broadening feature for Proton b compared to that for Proton a. It is reasonable to conclude that the Zn^{2+} ion interacts with the deprotonated thiol group for the formation of the Zn-MPA complex.

[1] R. Ravichandran in Applications of Ion Chromatography for Pharmaceutical and Biological Products (Eds: L. Bhattacharyya, J. S. Rohrer), John Wiley & Sons, Inc., Weinheim, Germany **2012**, Ch. 16.

[2] W. Wan, M. Zhang, M. Zhao, N. Rowell, C. Zhang, S. Wang, T. Kreouzis, H. Fan, W. Huang, K. Yu, Room-Temperature Formation of CdS Magic-Size Clusters in Aqueous Solutions Assisted by Primary Amines, *Nat. Commun*. **2020**, *11*, 4199.

[3] M. Zhao, Q. Chen, Y. Zhu, Y. Liu, C. Zhang, G. Jiang, M. Zhang, K. Yu, Precursor Compound Enabled Formation of Aqueous-Phase CdSe Magic-Size Clusters at Room Temperature, *Nano Res.* **2022**, *15*, 2634–2642.

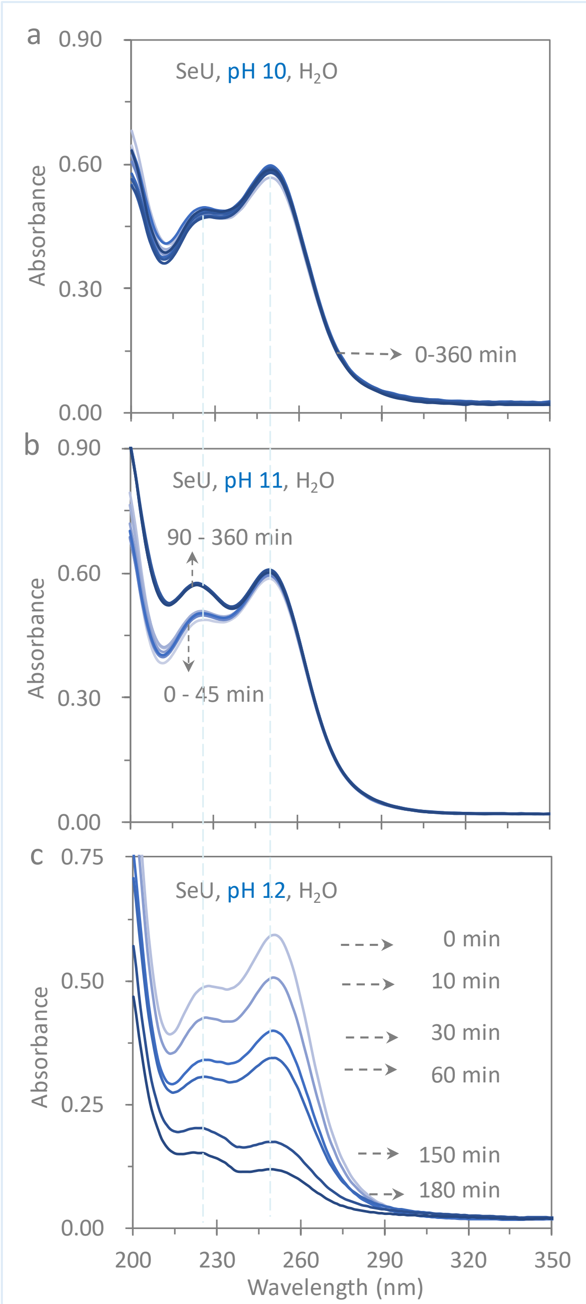

Figure S3-2. Hydrolysis of SeU at different pH explored by optical absorption spectroscopy. SeU was added to water with the pH value of 10 (a), 11 (b), and 12 (c), to resulting in the concentration of 4 mM. Ten samples were taken at 0, 5, 10, 20, 30, 45, 90, 150, 300, 360 min (a and b), and six at 0, 10, 30, 60, 150, 180 min (c). Each sample (50 µL) was then dispersed in 3.0 mL H_2O for the absorption measurement. It is evident that the hydrolysis of SeU occurs when the pH value is larger than 10. Following a previous study,[1] we propose the hydrolysis is $Se{=}C(NH_2)_2 + 2OH^- \Rightarrow Se^{2-} + 2H_2O + NH_2\text{-}CN$

[1] Y. Wang, Z. Liu, N. Huo, F. Li, M. Gu, X. Ling, Y. Zhang, K. Lu, L. Han, H. Fang, A. G. Shulga, Y. Xue, S. Zhou, F. Yang, X. Tang, J. Zheng, M. A. Loi, G. Konstantatos, W. Ma, Room-Temperature Direct Synthesis of Semi-conductive PbS Nanocrystal Inks for Optoelectronic Applications, *Nat. Commun.* **2019**, *10*, 5136.

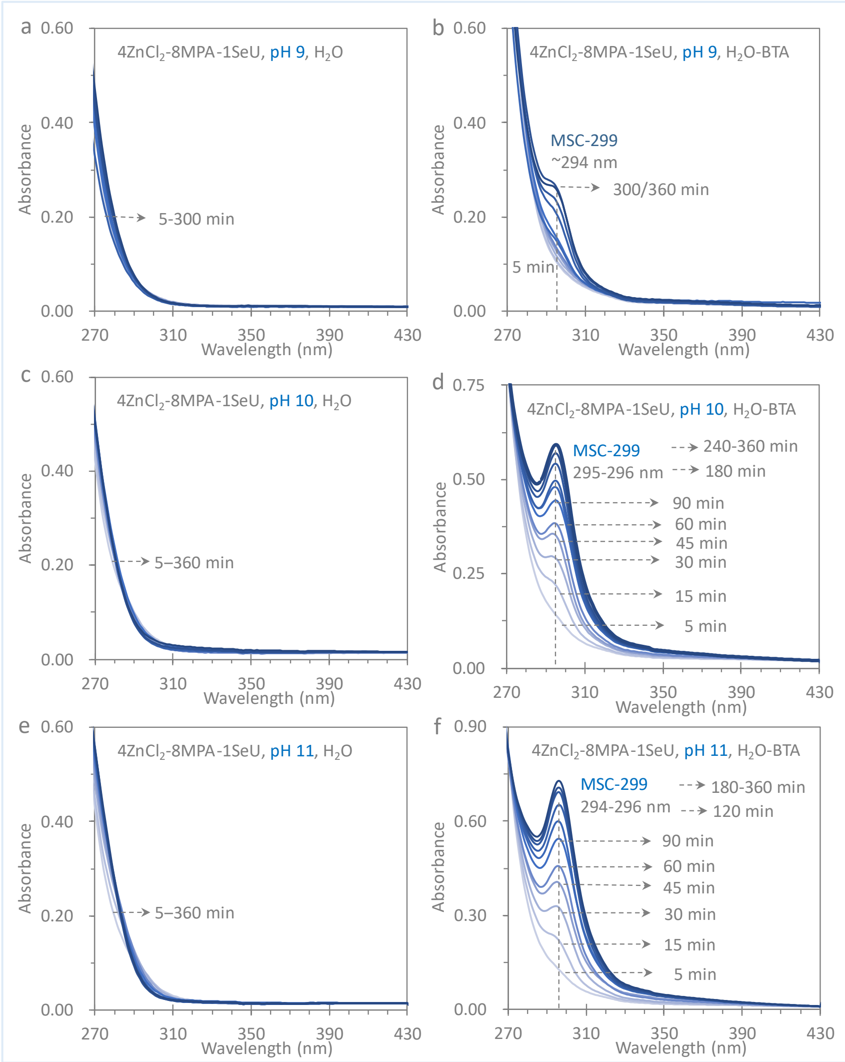

Figure S3-3. The effect of pH explored by optical absorption spectroscopy. The three reactions are similar to that for Figure 1 except pH of 9 (top panel a and b), 10 (middle panel c and d), and 11 (bottom panel e and f). Samples were extracted at 5, 15, 30, 45, 60, 90, 120, 180, 240, 300, and 360 min. Similarly, dispersions were prepared with an aliquot (100 µL) of each sample in 3.0 mL H_2O (left panel a, c, e) and in the mixture of 1.5 mL H_2O and 1.5 mL BTA (right panel b, d, f). The reactions are in the prenucleation stage. Although the hydrolysis of SeU does not occur with pH 10 (Figure S3-2), the PC-299 forms even in the pH 9 reaction (a). Thus, it is reasonable that the hydrolysis of SeU occurs at pH 9 due to the presence of Zn-MPA complex in the reaction.

Figure S3-4. Evolution of PC-299 in situ monitored by ^{1}H NMR and ex situ by optical absorption spectroscopy. The room-temperature reaction is that for Figure 1 but with a SeU concentration of 10 mM in D_2O (pH ~12 estimated by pH test paper). For the ^{1}H NMR spectra (a) measured at the eight reaction periods as indicated, the protons of the two CH_2 groups are labelled as Protons a and b, which are respectively close to the -COOH and -SH groups in MPA. For the absorption spectra (b), an aliquot (25 µL) of each of the eight samples (extracted from another identical reaction with the similar reaction periods) was dispersed in a mixture of 1.5 mL H_2O and 1.5 mL BTA. In Part c, the change of the chemical shift of Proton b (a) and the change of the absorbance of MSC-299 (b) are summarized. The former is from 0.001 to 0.025 ppm, and the latter is from 0.10 to 0.38. The presence of MSC-299 suggests the evolution of ZnSe PC-299 in the reaction. As well, the resonance signal of Proton b gradually shifts up-field and becomes sharper.

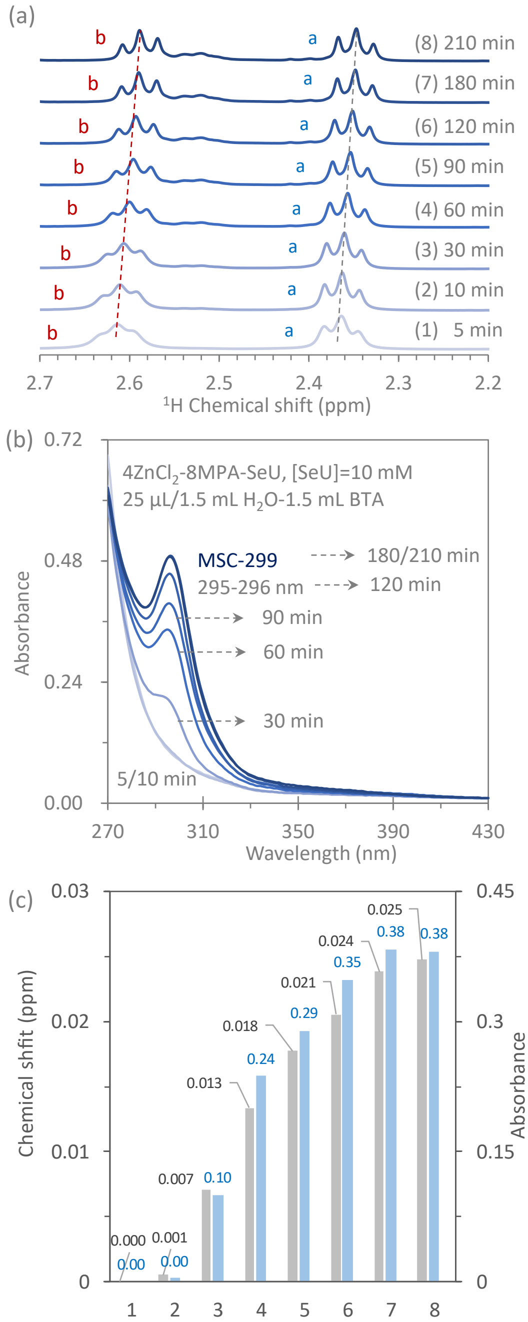

For Part a trace 1 (5 min), the resonance signal is at about 2.61 ppm for Proton b and 2.36 ppm for Proton a. For trace 8 (210 min), the resonance signal is at 2.59 ppm for Proton b and 2.35 ppm for Proton a. Proton b is relatively broad at 5 min, but becomes sharper gradually as 210 min. It is noteworthy that the Zn-MPA complex (Figure S3-1 Trace 5) displays 2.57 ppm for Proton b and 2.32 ppm for Proton a. For Part b, MSC-299 is not seen in the 5 and 10 min samples, and is seen in the remaining samples with an increase of OD within 180 min and becomes stable afterward (at 210 min monitored).

We argue that the Proton b signal is contributed by species such as free MPA, the Zn-MPA complex, the monomers and fragments, and PC-299. Along the reaction, the resonance signal of Proton b persistently shifts and becomes as sharp as that of Proton a. This change is related to the formation of Zn-Se covalent bonds, which results in the release of free MPA. Therefore, the averaged chemical environment of MPA becomes more closer to that of free MPA.

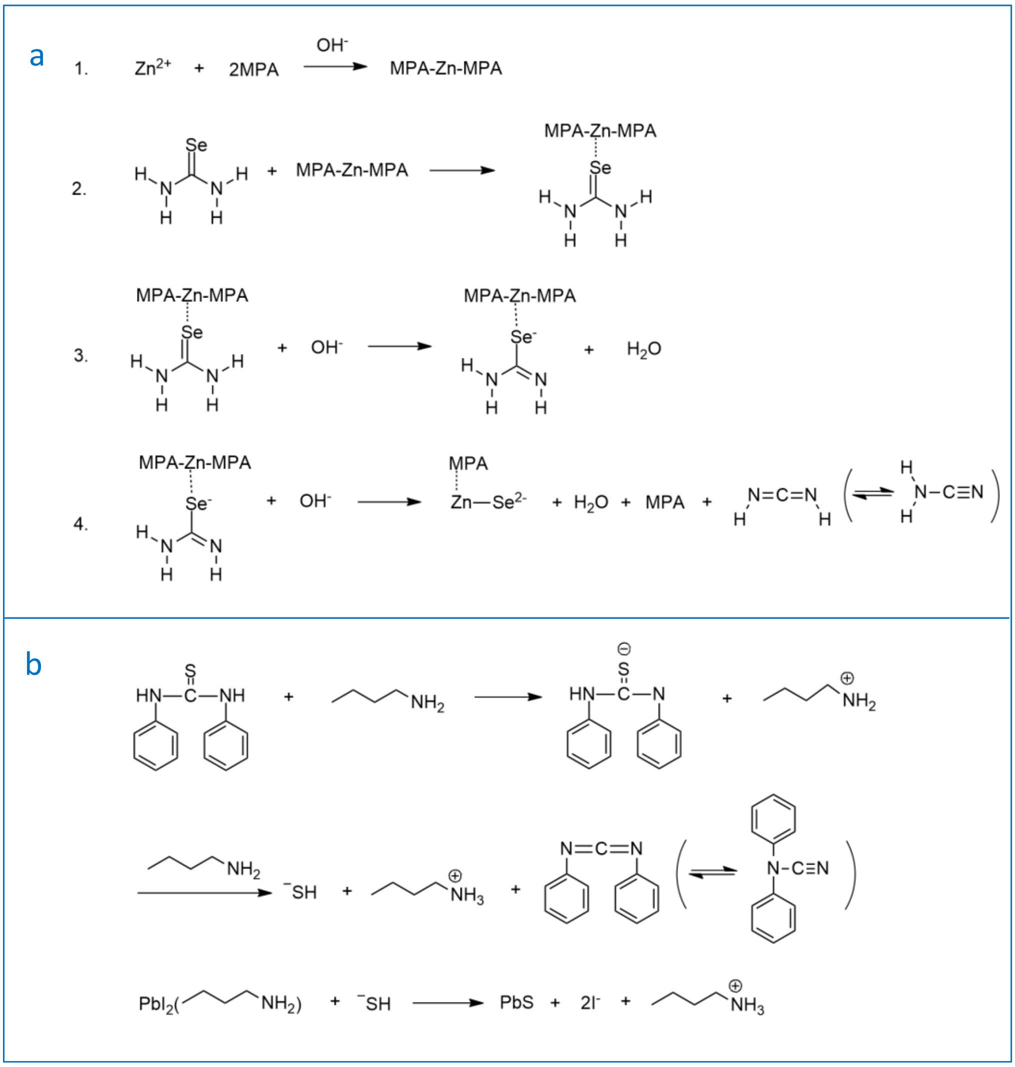

Figure S3-5. Reactions proposed for the Zn-Se covalent bond formation (a) following those for the Pb-S covalent bond formation (b).[1] In Part a, the aqueous-phase formation of Zn-MPA complex is Step 1, supported by ^{1}H NMR shown in Figure S3-1. The coordination between SeU and the Zn-MPA complex is Step 2. Steps 3 and 4 are for the hydrolysis of the activated SeU, which can occur at a low pH such as 9 (Figures S3-2 and S3-3). The Zn-Se covalent bond formation is accelerated at high pH (Figures S3-3 and S3-4). Part b is reproduced from a previously report, which addresses the BTA-assisted decomposition of diphenyl thiourea in dimethyl formamide (DMF) for the room-temperature evolution of PbS QDs. In a side note, it is of help to point out that for the present study of ZnSe, BTA assists the PC to MSC-299 isomerization (Step 2) only, while MPA enables the formation of Zn-Se covalent bonds. So, the surface ligand of MSC-299 is MPA mainly. Conventional mass spectrometry (MS) does not provide ligand information due to the detachment of ligands, such as laser-desorption-ionization (LDI) MS and matrix-assisted laser desorption/ionization time-of-flight (MALDI-TOF) MS.[2-4]".

[1] Y. Wang, Z. Liu, N. Huo, F. Li, M. Gu, X. Ling, Y. Zhang, K. Lu, L. Han, H. Fang, A. G. Shulga, Y. Xue, S. Zhou, F. Yang, X. Tang, J. Zheng, M. A. Loi, G. Konstantatos, W. Ma, Room-

Temperature Direct Synthesis of Semi-conductive PbS Nanocrystal Inks for Optoelectronic Applications, *Nat. Commun.* **2019**, *10*, 5136.
[2] Y. Wang, Y. Liu, Y. Zhang, F. Wang, P. J. Kowalski, H. W. Rohrs, R. A. Loomis, M. L. Gross, W. E. Buhro, Isolation of the Magic-Size CdSe Nanoclusters [$(CdSe)_{13}$(n-octylamine)$_{13}$] and [$(CdSe)_{13}$(oleylamine)$_{13}$], *Angew. Chem. Int. Ed.* **2012**, *51*, 6154–6157.
[3] S. Dolai, P. R. Nimmala, M. Mandal, B. B. Muhoberac, K. Dria, A. Dass, R. Sardar, Isolation of Bright Blue Light-Emitting CdSe Nanocrystals with 6.5 kDa Core in Gram Scale: High Photoluminescence Efficiency Controlled by Surface Ligand Chemistry, *Chem. Mater.* **2014**, *26*, 1278–1285.
[4] L. Xie, Y. Shen, D. Franke, V. Sebastian, M. G. Bawendi, K. F. Jensen, Characterization of Indium Phosphide Quantum Dot Growth Intermediates using MALDI-TOF Mass Spectrometry. *J. Am. Chem. Soc.* **2016**, *138*, 13469–13472.

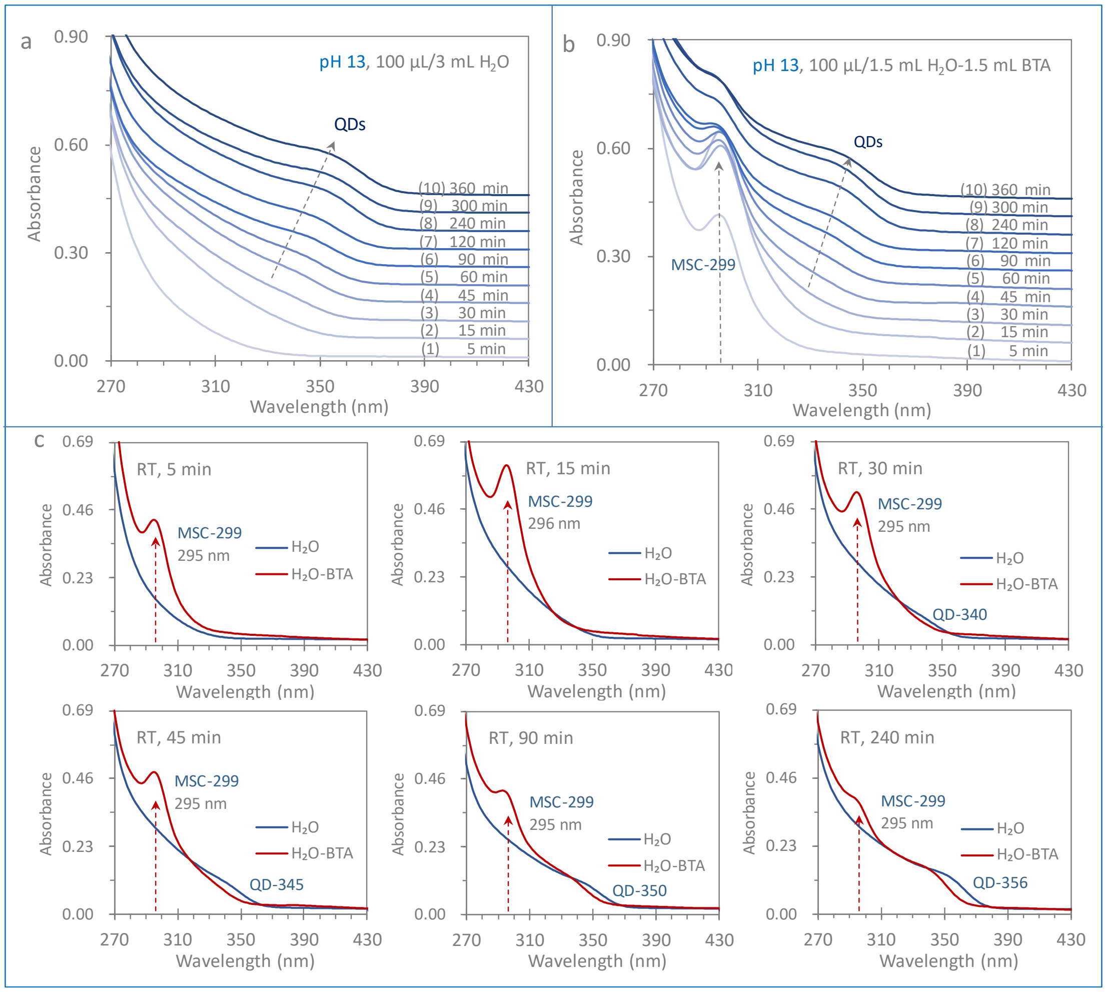

Figure S3-6. Optical absorption spectra of the 11 samples from the Figure 3 room-temperature reaction with pH 13. The 11 samples were taken within the period of 360 min as indicated. An aliquot (100 µL) of each sample was dispersed into 3.0 mL H_2O (a) and the mixture of 1.5 mL H_2O and 1.5 mL BTA (b). Parts c highlights the samples collected at 5, 15, 30, 45, 90, and 240 min. It is evident that when the nucleation and growth of QDs take place, the amount of PC-299 in the reaction decreases.

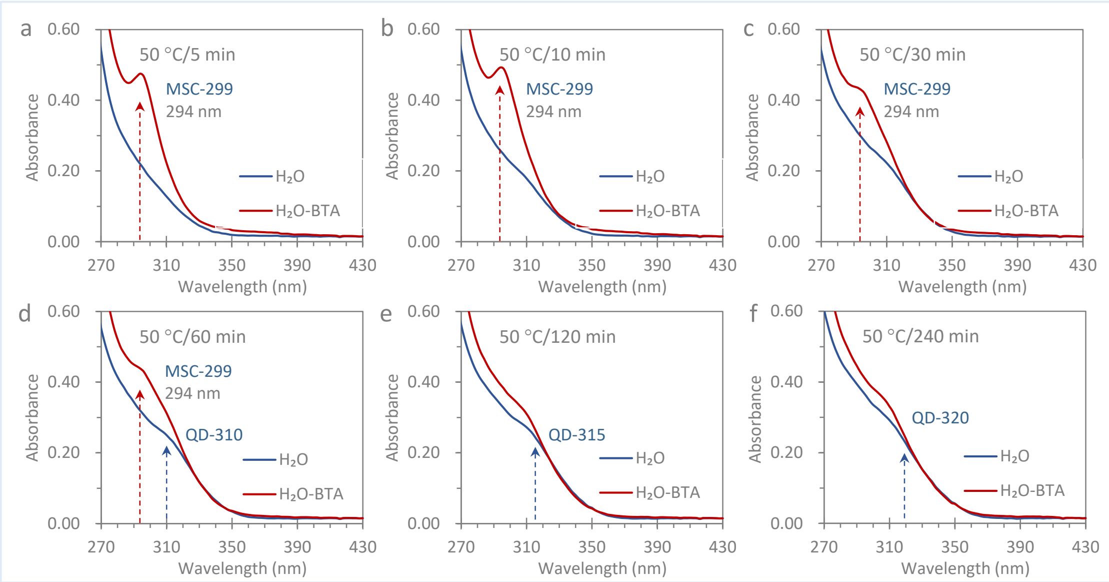

Figure S4-1. Optical absorption spectra of six samples from the Figure 1 reaction at 50 °C. Samples were taken at 5 (a), 10 (b), 30 (c), 60 (d), 120 (e), and 240 min (f). An aliquot (100 µL) of each sample was dispersed in 3.0 mL H_2O (blue traces) and in the mixture of 1.5 mL H_2O and 1.5 mL BTA (red traces). In the periods of 5 to 60 min (a to d). ZnSe PC-299 forms in the reaction and disappears almost completely within 60 min (d). The size of QDs obtained is relatively small.

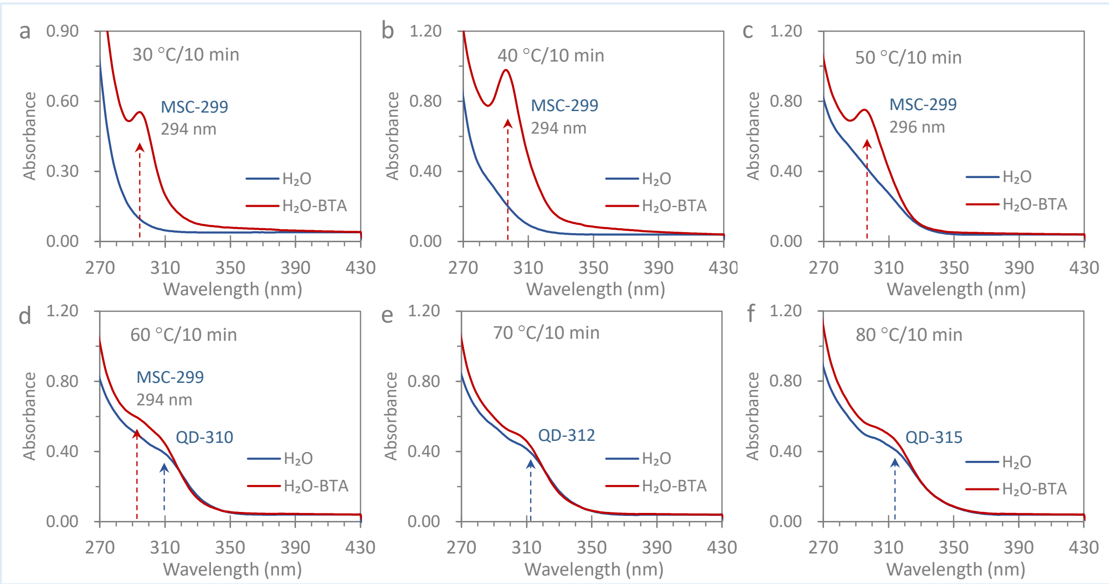

Figure S4-2. Optical absorption spectra of six samples from the Figure 1 reaction from 30 to 80 °C. The reaction was heated with steps of 10 °C, and samples were extracted at each step after 10 min had elapsed. For the absorption measurement, each sample (100 µL) was dispersed in 3.0 mL of H_2O (blue traces) and in the mixture of 1.5 mL of H_2O and 1.5 mL BTA (red traces). PC-299 forms and disappears completely at 60 °C. The nucleation and growth of ZnSe QDs starts at 40 °C (b). Relatively small-size QDs are obtained.

Figure S4-3. MALDI-TOF MS of a purified prenucleation stage sample. With 2,5-dihydroxybenzoic acid (DHB) as the matrix, the sample that contains mostly ZnSe PC-299 displays a peak at m/z of 3221 in the detection range from 3000 to 4000 Da. A previous study reports ~3350 Da (with α-Cyano-4-hydroxycinnamic acid (CHCA) as the matrix) for purified ZnSe PC-299 but from a non-aqueous phase synthesis.[1] The accurate composition for the PC and the composition, size, and structure for the MSC are not available, which are the ongoing challenge.[2-5] For example, CdS MSC-324 was first reported in 1984,[6] and another research group reported CdS MSC-313 and MSC-324 in 2017.[7] With a large-scale production of ~12 g for MSC-324 in 2018, the number of Cd atoms per MSC was estimated to be between 17 to 32 atoms.[8] In 2019, a composition of $Cd_{37}S_{20}$ for MSC-313 and MSC-324 was suggested,[9] but $Cd_{37}S_{18}$ in 2022.[10]

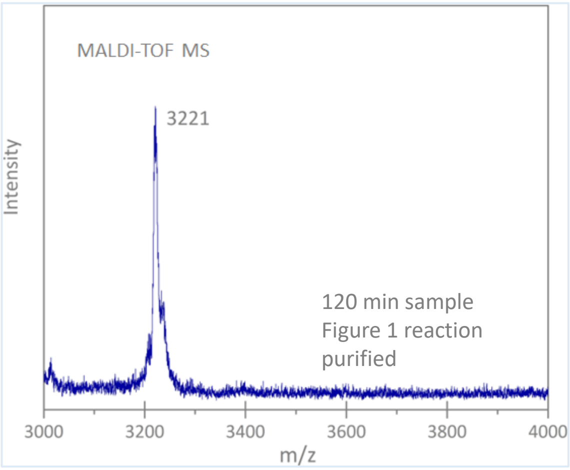

[1] X. Yang, M. Zhang, Q. Shen, Y. Li, C. Luan, K. Yu, The Precursor Compound of Two Types of ZnSe Magic-Size Clusters, *Nano Res.* **2022**, *15*, 465–474.
[2] M. Zanella, A. Z. Abbasi, A. K. Schaper, W. J. Parak, Discontinuous Growth of II-VI Semiconductor Nanocrystals from Different Materials, *J. Phys. Chem. C* **2010**, *114*, 6205.
[3] L. Xie, Y. Shen, D. Franke, V. Sebastian, M. G. Bawendi, K. F. Jensen, Characterization of Indium Phosphide Quantum Dot Growth Intermediates Using MALDI-TOF Mass Spectrometry, *J. Am. Chem. Soc.* **2016**, *138*, 13469.
[4] C. Palencia, K. Yu, K. Boldt, The Future of Colloidal Semiconductor Magic-Size Clusters, *ACS Nano* **2020**, *14*, 1227−1235.
[5] S. Busatto, C. M. Donega, Magic-Size Semiconductor Nanostructures: Where Does the Magic Come from? *ACS Mater. Au* **2022**, *2*, 237–249.
[6] A. Fojtik, H. Weller, U. Koch, A. Henglein, Photo-Chemistry of Colloidal Metal Sulfides 8. Photo-Physics of Extremely Small CdS Particles: Q-State CdS and Magic Agglomeration Numbers, *Ber. Bunsenges. Phys. Chem.* **1984**, *88*, 969–977.
[7] D. R. Nevers, C. B. Williamson, T. Hanrath, R. D. Robinson, Surface Chemistry of Cadmium Sulfide Magic-Sized Clusters: A Window into Ligand-Nanoparticle Interactions, *Chem. Commun*. **2017**, *53*, 2866–2869.
[8] D. R. Nevers, C. B. Williamson, B. H. Savitzky, I. Hadar, U. Banin, L. F. Kourkoutis, T. Hanrath, R. D. Robinson, Mesophase Formation Stabilizes High-Purity Magic-Sized Clusters, *J. Am. Chem. Soc.* **2018**, *140*, 3652–3662.
[9] C. B. Williamson, D. R. Nevers, A. Nelson, I. Hadar, U. Banin, T. Hanrath, R. D. Robinson, Chemically Reversible Isomerization of Inorganic Clusters, *Science* **2019**, *363*, 731–735.
[10] H. Han, S. Kallakuri, Y. Yao, C. B. Williamson, D. R. Nevers, B. H. Savitzky, R. S. Skye, M. Xu, O. Voznyy, J. Dshemuchadse, L. F. Kourkoutis, S. J. Weinstein, T. Hanrath, R. D. Robinson, Multiscale Hierarchical Structures from a Nanocluster Mesophase, *Nat. Mater.* **2022**, *21*, 518–525.

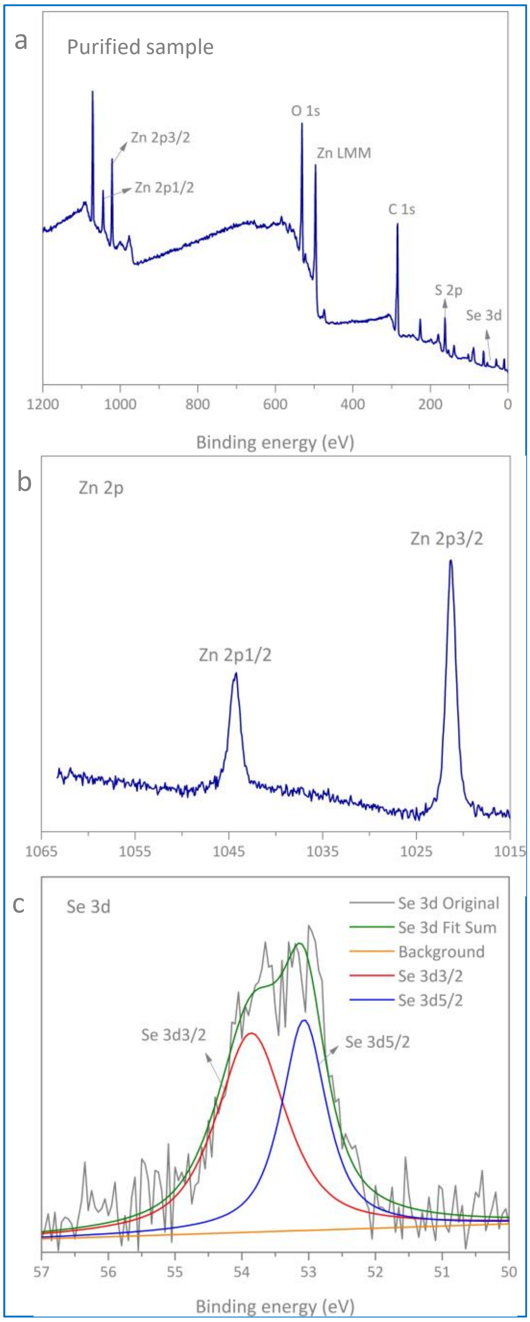

Figure S4-4. XPS of the purified prenucleation stage sample. Part a is a survey scan presented in 0 to 1200 eV. Parts b and c are respectively for Zn 2p (1015 to 1065 eV), and Se 3d (50 to 57 eV).[1] Zn, Se, and S, together with C and O are detected, in agreement with that MPA is the ligand that binds to the core of ZnSe.

[1] K. Yu, A. Hrdina, J. Ouyang, D. Kingston, X. Wu, D. M. Leek, X. Liu, C. Li, Ultraviolet $ZnSe_{1-x}S_x$ Gradient-Alloyed Nanocrystals via a Noninjection Approach, *ACS Appl. Mater. Interfaces* **2012**, *4*, 4302–4311.

Figure S4-5. XRD (a) and TEM (b and c) of our two ZnSe samples (purified). The PC-299 sample is the 120 min same from the Figure 1 reaction. The QD-347 sample is from the Figure 3 reaction with the period of 90 min. The XRD standard card of wurtzite (Trace 1) and zinc blende (Trace 4) of the bulk ZnSe is shown in Part a, together with Trace 2 for PC-299 and Trace 3 for QD-347. QD-347 has a cubic structure, similar to that of Trace 4 with the diffraction peak of (111) plane at 28.2°, (220) at 46.6°, and (311) at 53.9°. ZnSe PC-299 may have a TEM size of ~ 3 nm (b). The QD-347 TEM image (c) shows distinct lattice fringes (as shown in the inset). TEM does not provide reliable size information for small-size QDs, MSCs, and PCs.[1-5]

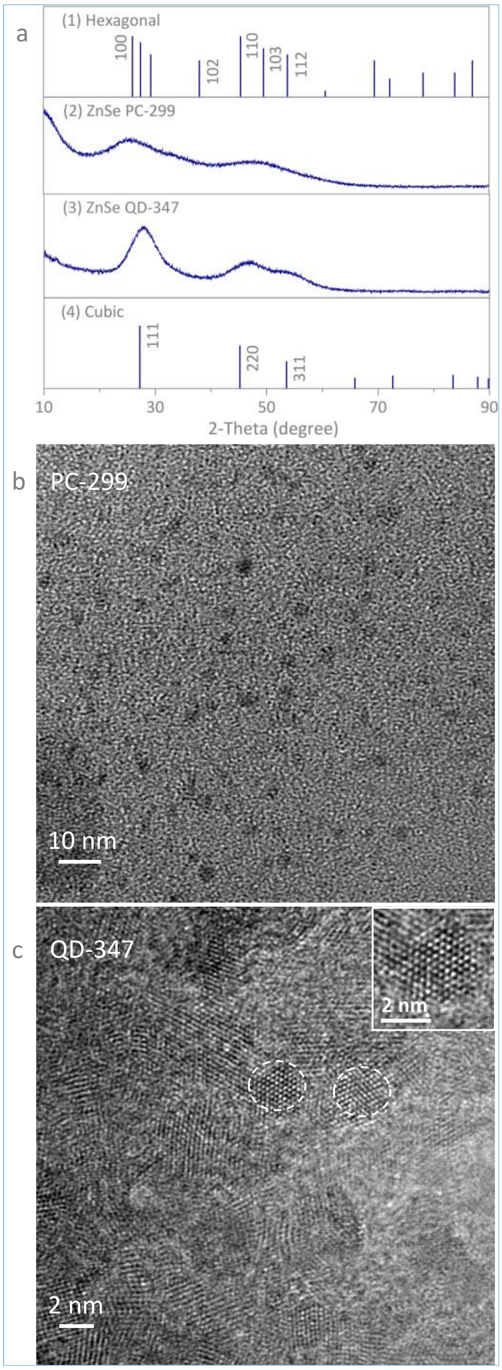

[1] L. Xie, Y. Shen, D. Franke, V. Sebastian, M. G. Bawendi, K. F. Jensen, Characterization of Indium Phosphide Quantum Dot Growth Intermediates Using MALDI-TOF Mass Spectrometry, *J. Am. Chem. Soc.* **2016**, *138*, 13469.

[2] Y. Kwon, J. Oh, E. Lee, S. H. Lee, A. Agnes, G. Bang, J. Kim, D. Kim, S. Kim, Evolution from Unimolecular to Colloidal-Quantum-Dot-Like Character in Chlorine or Zinc Incorporated InP Magic Size Clusters, *Nat. Commun*. **2020**, *11*, 3127.

[3] A. S. Mule, S. Mule, S. Mazzotti, A. A. Rossinelli, M. Aellen, P. T. Prins, J. C. van der Bok, S. F. Solari, Y. M. Glauser, P. V. Kumar, A. Riedinger, D. J. Norris, Unraveling the Growth Mechanism of Magic-Sized Semiconductor Nanocrystals, *J. Am. Chem. Soc*. **2021**, *143*, 2037–2048.

[4] C. Palencia, K. Yu, K. Boldt, The Future of Colloidal Semiconductor Magic-Size Clusters, *ACS Nano* **2020**, *14*, 1227–1235.

[5] S. Busatto, C. M. Donega, Magic-Size Semiconductor Nanostructures: Where Does the Magic Come from? *ACS Mater. Au* **2022**, *2*, 237–249.

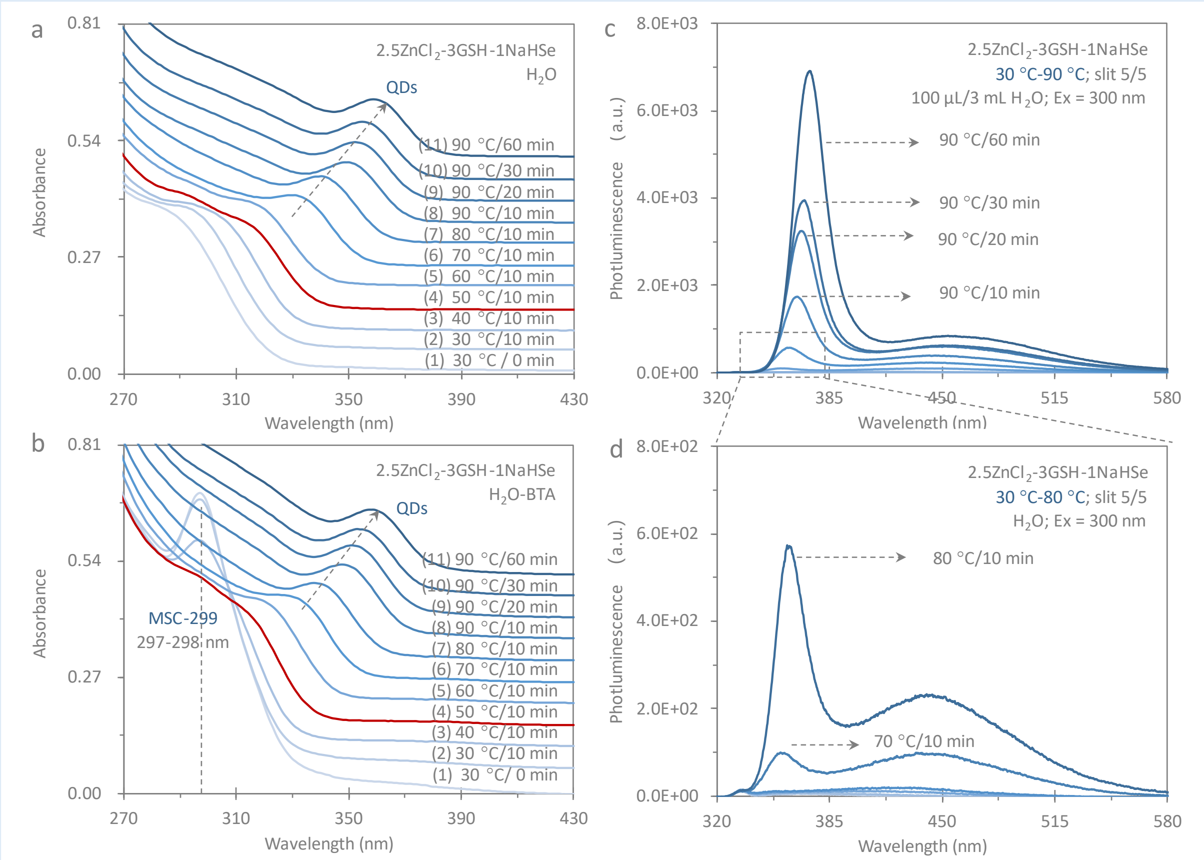

Figure S5-1. The optical absorption (a and b) and photoluminescence (PL) (c and d) spectra from the 11 samples extracted from the Figure 5 reaction. The reaction is 2.5ZnCl$_2$-3GSH-1NaHSe with a Se concentration of 4 mM and pH 11.5. The reaction temperature was increased from 30 to 90 °C. An aliquot (100 µL) of each sample was dispersed into 3.0 mL H_2O (a, c and d) and into the mixture of 1.5 mL H_2O and 1.5 mL BTA (b). Parts c shows the PL spectra, with those from Samples 1 (30 °C) to 7 (80 °C) in Part d. PC-299 forms and disappears completely at 50 °C; the absorption and emission spectra of Sample 4 are highlighted in red in Parts a and b, respectively. The absorption broadens the most for the 50 °C sample. In a side note, we would like to point out that in previously-reported, organic-phase reactions,[1-7] the thermally-induced fragmentation of reaction intermediates could have existed. Thus, the optical absorption spectra could be revisited, with attention to peaks on the shorter wavelength side of the first excitonic peak.[4-7]

[1] D. C. Gary, M. W. Terban, S. J. L. Billinge, B. M. Cossairt, Two-Step Nucleation and Growth of InP Quantum Dots via Magic-Sized Cluster Intermediates, *Chem. Mater.* **2015**, *27*, 1432–1441.

[2] A. Ritchhart, B. M. Cossairt, Templated Growth of InP Nanocrystals with a Polytwistane Structure, *Angew. Chem. Int. Ed.* **2018**, *57*, 1908–1912.

[3] M. R. Friedfeld, D. A. Johnson, B. M. Cossairt, Coversion of InP Clusters to Quantum Dots, *Inorg. Chem.* **2019**, *58*, 803–810.

[4] C. B. Murray, D. J. Norris, M. G. Bawendi, Synthesis and Characterization of Nearly Monodisperse CdE (E = S, Se, Te) Semiconductor Nanocrystallites *J. Am. Chem. Soc.* **1993**, *115*, 8706–8715.

[5] Z. A. Peng, X. Peng, Nearly Monodisperse and Shape-Controlled CdSe Nanocrystals via

Alternative Routes: Nucleation and Growth, *J. Am. Chem. Soc.* **2002**, *124,* 3343–3353.
[6] Y. A. Yang, H. Wu, K. R. Williams, Y. C. Cao, Synthesis of CdSe and CdTe Nanocrystals without Precursor Injection, *Angew. Chem. Int. Ed.* **2005**, *44*, 6712–6715.
[7] Z. Jiang, D. F. Kelley, Role of Magic-Sized Clusters in the Synthesis of CdSe Nanorods, *ACS Nano* **2010**, *4*, 1561−1572.

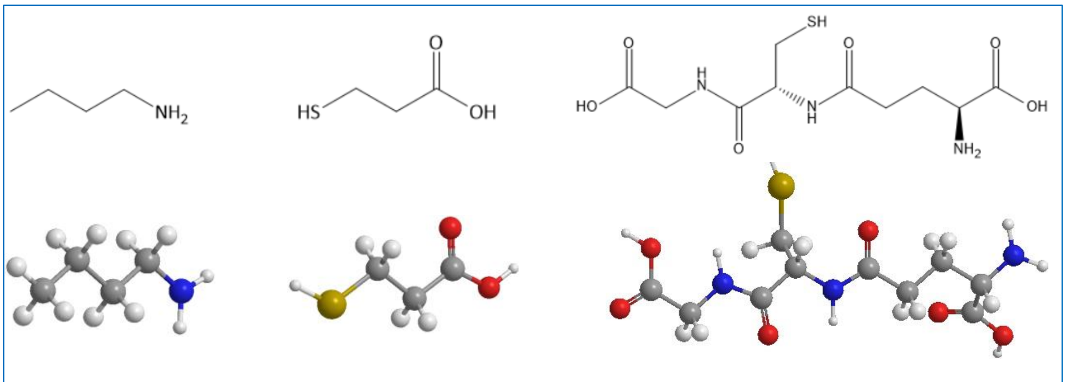

Figure S5-2. The chemical structures of BTA, MPA and GSH. The atoms have the color of blue (N), yellow (S), red (O), gary (C), and white (H). The reactions between Zn/MPA and SeU (Figure 1) and between Zn/GSH and NaHSe (Figure 5) are different. They have similar pathways of the nucleation and growth of aqueous-phase ZnSe QDs, particularly regarding the formation of PC-299 (Step 1). In a side note, we would like to point out that SeU is a commercially available compound of selenocarbonyls, while NaHSe has to be freshly prepared from a reaction of Se + $NaBH_4$.[1] When the solution becomes clearly without visible Se powder, NaHSe is used directly without purification. We think, it is not accurate enough to estimate the NaHSe amount based on the Se amount, due to the complication of the reaction side product H_2Se.[1] It is apparent that the reactivity of SeU is lower than that of NaHSe. SeU and NaHSe have distinct chemical structures. The chemical structure plays a significant role on the reactivity, which can be further affected by experimental variables such as concentrations, pH, and temperatures. Thus, the variables of concentrations and feed molar ratios of Zn to Se are particularly addressed in Scheme 1. In the presence of BTA, optically transparent PC-299 produced from the former and latter reactions is forced to transform absorbing MSC-299 (Step 2). Here, we would like to point out again that aqueous-phase approaches to semiconductor magic-size clusters (MSCs) and quantum dots (QDs) that are free of heavy metal have remained relatively unexplored. We report the first selective approach to ZnSe MSCs and QDs in aqueous solutions at room temperature. The former exhibits a sharp optical absorption peaking at 299 nm, thus labelled MSC-299, while the latter displays a relatively broad absorption peaking in the range from 310 to 360 nm. We argue that the synthetic selectivity is enabled by a special reaction intermediate formed, which is optically transparent at 299 nm and to longer wavelengths. This intermediate either transforms to MSC-299 via intra-molecular reorganization, or fragments to assist the development of QDs. This intermediate forms in various Zn and Se reaction systems, providing unambiguous evidence that the presence of reaction intermediates prior to nucleation warrants thorough consideration as nucleation theory advances.

[1] D. L. Klayman, T. S. Griffin, Reaction of Selenium with Sodium Borohydride in Protic Solvents. A Facile Method for the Introduction of Selenium into Organic Molecules, *J. Am. Chem. Soc.* **1973**, *95*, 197–199.

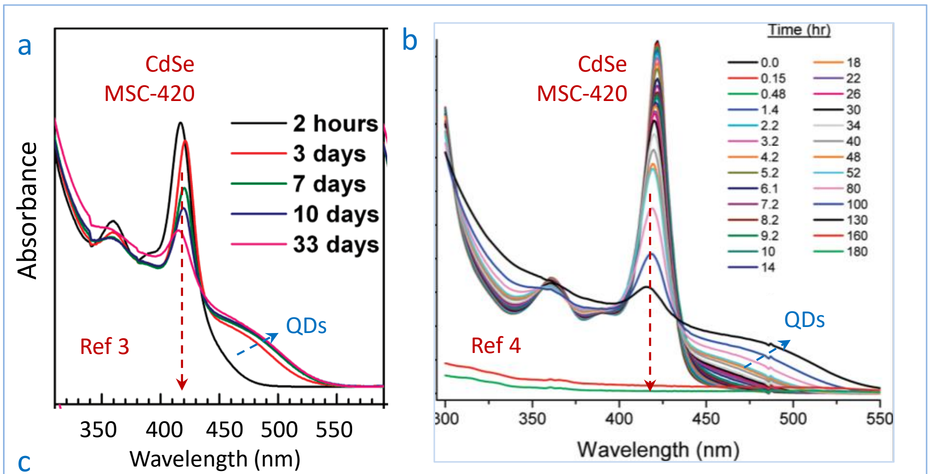

c

Refs (Year)	CdE MSCs	Cd and E sources
1 (2020)	CdS MSC-360	$2CdCl_2$-8MPA-1thiourea; [thiourea]=2 mM
2-5 (2010-2012)	CdSe MSC-420	$4CdSO_4$-35.2Cys-$1Na_2SeSO_3$; [Se]=0.375 mM
6-8 (2017-2019)	CdSe MSC-422	$2Cd(OH)_2$-8Cys-$1Na_2SeSO_3$; [Se]=16 mM
9 (2022)	CdSe MSC-422	$2Cd(OH)_2$-8Cys-$1Na_2SeSO_3$; [Se]=14 mM
10 (2022)	CdSe MSC-420	$2CdCl_2$-8MPA/8Cys-1SeU; [SeU]=5 mM

Figure S6. Aqueous-phase CdSe MSC-420 derived from Ref 3 (a) and Ref 4 (b) mentioned in Table (c) for literature reports of aqueous-phase CdE MSCs.[1-10] Part a shows the time-dependent evolution of UV-vis absorption spectra for Cysteine methylester (CysME)-capped CdSe MSC-420. Part b shows the absortpion spectra of CdSe MSC-420 after diluted into an aqueous solution containing 100 mM NaOH. The probably related change between MSCs and QDs has not been addressed in these published papers. We argue that the decrease of MSC-420 and the increase of QDs is related to the MSC-420 to PC-420, which fragments and QDs grow. [Part a reproduced from Figure 5a of Ref 3. Copyright 2010 American Chemical Society. Part b reproduced from Figure 1 of Ref 4. Copyright 2011 American Chemical Society].

[1] W. Wan, M. Zhang, M. Zhao, N. Rowell, C. Zhang, S. Wang, T. Kreouzis, H. Fan, W. Huang, K. Yu, Room-Temperature Formation of CdS Magic-Size Clusters in Aqueous Solutions Assisted by Primary Amines. *Nat. Commun*. **2020**, *11*, 4199.
[2] Y. S. Park, A. Dmytruk, I. Dmitruk, A. Kasuya, Y. Okamoto, N. Kaji, M. Tokeshi, Y. Baba. Aqueous Phase Synthesized CdSe Nanoparticles with Well-Defined Numbers of Constituent Atoms. *J. Phys. Chem. C* **2010**, *114*, 18834–18840.
[3] Y. S. Park, A. Dmtruk, I.Dmitruk, A. Kasuya, M. Takeda, N. Ohuchi, Y. Okamoto, N. Kaji, M. Tokeshi, Y. Baba, Size-Selective Growth and Stabilization of Small CdSe Nanoparticles in Aqueous Solution. *ACS Nano* **2010**, *4*, 121–128.

[4] J. S. Baker, J. S. Nevins, K. M. Coughlin, L. A. Colón, D. F. Watson, Influence of Complex-Formation Equilibria on the Temporal Persistence of Cysteinate-Functionalized CdSe Nanocrystals in Water. *Chem. Mater.* **2011**, *23*, 3546–3555.
[5] Y.-S. Park, Y. Okamoto, N., Kaji, M. Tokeshi, Y. Baba, Aqueous Phase Synthesized CdSe Magic-Sized Clusters: Solution Composition Dependence of Adsorption Layer Structure. *J. Nanosci. Nanotechnol.* **2012**, *12*, 539–546.
[6] T. Kurihara, Y. Noda, K. Takegoshi, Quantitative Solid-State NMR Study on Ligand-Surface Interaction in Cysteine-Capped CdSe Magic-Sized Clusters. *J. Phys. Chem. Lett.* **2017**, *8*, 2555–2559.
[7] T. Kurihara, A. Matano, Y. Noda, K. Takegoshi, Rotational Motion of Ligand-Cysteine on CdSe Magic-Sized Clusters. *J. Phys. Chem. C* **2019**, *123*, 14993–14998.
[8] T. Kurihara, Y. Noda, K. Takegoshi, Capping Structure of Ligand–Cysteine on CdSe Magic-Sized Clusters. *ACS Omega* **2019**, *4*, 3476–3483.
[9] P. Wang, Q. Yang, C. Xu, B. Wang, H. Wang, J. Zhang, Y. Jin, Magic-Sized CdSe Nanoclusters for Efficient Visible-Light-Driven Hydrogen Evolution, *Nano Res.* **2022**, *15*, 3106–3113.
[10] M. Zhao, Q. Chen, Y. Zhu, Y. Liu, C. Zhang, G. Jiang, M. Zhang, K. Yu, Precursor Compound Enabled Formation of Aqueous-Phase CdSe Magic-Size Clusters at Room Temperature, *Nano Res.* **2022**, *15*, 2634–2642.

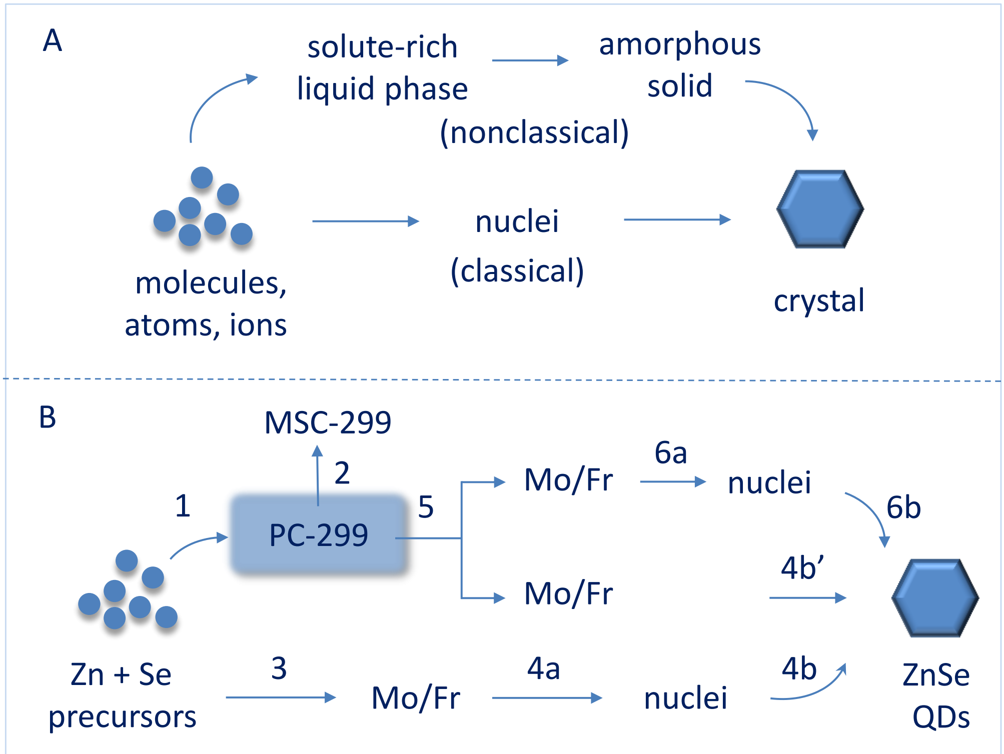

Scheme S1. The schematical drawing of the pathways of crystallization from aqueous environments for non-semiconductors (A) and for ZnSe QDs (B). The shape and size scale are not considered. Part A contains the nonclassical and classical crystallization pathways,[1,2] with the former containing multiple steps including a dense liquid phase,[3] prenucleation clusters,[4] or an amorphous phase claimed.[5] "Nonclassical crystallization–involving initial formation of an amorphous phase–occurs often in protein, organic, and inorganic crystallization processes."[6] Part B is the model proposed for aqueous-phase semiconductor ZnSe QDs. The formation of reaction intermediates in the prenucleation stage is similar in both aqueous-phase and organic-phase syntheses, with PC-299 analogue to the terms such as "the ultrasmall molecular intermediate species" and "nanoclusters" and "clusters" referred elsewhere.[7-12] "The relationship between the nanoclusters observed during the nanoparticle synthesis and magic sized clusters has been long recognized."[7] "Furthermore, nanoclusters, the ultrasmall molecular intermediate species with unique electronic and geometric structures, have been identified during the colloidal synthesis of metal, metal oxide, and semiconductor nanocrystals."[9] Whether the non-semiconductor system (Part A) has species similar to PC-299 (Part B) is unknown.

[1] M. Jehannin, A. Rao, H Cölfen, New Horizons of Nonclassical Crystallization, *J. Am. Chem. Soc.* **2019**, *141*, 10120–10136.

[2] J. J. De Yoreo, P. U. P. A. Gilbert, N. A. J. M. Sommerdijk, R. L. Penn, S. Whitelam, D. Joester, H. Zhang, J. D. Rimer, A. Navrotsky, J. F. Banfield, A. F. Wallace, F. M. Michel, F. C. Meldrum, H. Cölfen, P. M. Dove, Crystallization by Particle Attachment in Synthetic, Biogenic, and Geologic Environments, *Science* **2015**, *349*, aaa6760.

[3] N. D. Loh, S. Sen, M. Bosman, S. F. Tan, J. Zhong, C. A. Nijhuis, P. Král, P. Matsudaira, U. Mirsaidov, Multistep Nucleation of Nanocrystals in Aqueous Solution, *Nat. Chem.* **2017**, *9*, 77−82.

[4] D. Gebauer, A. Völkel, H. Cölfen, Stable Prenucleation Calcium Carbonate Clusters, *Science* **2008**, *322*, 1819−1822.

[5] J. Yang, J. Koo, S. Kim, S. Jeon, B. K. Choi, S. Kwon, J. Kim, B. H. Kim, W. C. Lee, W. B. Lee, H. Lee, T. Hyeon, P. Ercius, J. Park, Amorphous-Phase-Mediated Crystallization of Ni Nanocrystals Revealed by High-Resolution Liquid-Phase Electron Microscopy, *J. Am. Chem. Soc.* **2019**, *141*, 763−768.

[6] L. Houben, H. Weissman, S. G. Wolf, B. Rybtchinski, A Mechanism of Ferritin Crystallization Revealed by Cryo-STEM Tomography, *Nature* **2020**, *579*, 540–543.

[7] J. Lee, J. Yang, S. G. Kwon, T. Hyeon, Nonclassical Nucleation and Growth of Inorganic Nanoparticles, *Nat. Rev. Mater.* **2016**, *1*, 16034.

[8] C. Palencia, K. Yu, K. Boldt, The Future of Colloidal Semiconductor Magic-Size Clusters, *ACS Nano* **2020**, *14*, 1227−1235.

[9] W. Baek, H. Chang, M. S. Bootharaju, J. H. Kim, S. Park, T. Hyeon, Recent Advances and Prospects in Colloidal Nanomaterials, *JACS Au* **2021**, *1*, 1849−1859.

[10] L. He, C. Luan, N. Rowell, M. Zhang, X. Chen, K. Yu, Transformations Among Colloidal Semiconductor Magic-Size Clusters, *Acc. Chem. Res.* **2021**, *54*, 776 – 786.

[11] Y. Li, N. Rowell, C. Luan, M. Zhang, X. Chen, K. Yu, A Two-Pathway Model for the Evolution of Colloidal Compound Semiconductor Quantum Dots and Magic-Size Clusters, *Adv. Mater.* **2022**, 2107940.

[12] A. Loiudice, R. Buonsanti, Reaction Intermediates in the Synthesis of Colloidal Nanocrystals, *Nat. Synth.* **2022**, *1*, 344–351.

Table S3. Examples reported about nonclassical crystallization in aqueous solutions.

Refs	Systems	Crystallization	Comments
1	$CaCO_3$	Potentiometric titration assay: • stable prenucleation-stage clusters • amorphous $CaCO_3$	• The cluster has a hydrodynamic diameter of ~2 nm • The cluster size distribution and structure remain unknown. • How these cluster form critical nucleic is unknown.
2	Au NCs	In situ TEM: • gold-rich liquid phase • amorphous gold nanoclusters	• Nanoclusters with low crystallinity cannot be seen. • Ag NCs have a similar same crystallization process
3	Pt NCs	In situ Liquid cell-TEM: • metal-rich liquid phase • "cluster-cloud" intermediate state • nucleus forms in the cluster-cloud	• The amount of "~1.0 nm ultrasmall clusters" within the cluster-cloud is unknown. • Conditions that the cluster-cloud state dominate are unknown.
4	glucose isomerase	LCM-DIM: • mesoscopic cluster formation • crystalline phase formation	• whether the clusters are an absolute requirement for nucleation is unknown.
5	Ibuprofen	Potentiometric titration assay: • dense liquid phase • nucleation of a crystalline phase	• The crystal evolution cannot be observed, and this process was inferred indirectly. • Whether different pathways coexist is unknown.
6	Ibuprofen	Cryo-TEM: • aggregates of varying density and order. • nucleated phases	• Multiple crystallization modes in the crystallization process. • How to control different evolution pathways is not addressed.

noninvasive laser confocal differential interference contrast microscopy (LCM-DIM)

Structural visualization for the intermediate is challenging. TEM has inherent limitation due to resolution and local information from a limited area. For example, the authors claimed in Ref 4 (with LCM-DIM) a nonclassical crystallization process of glucose isomerase, while with TEM (in *Nature* **2018**, *556*, 89–94) that "we do not identify a metastable dense liquid as the precursor to the crystalline state" and "the rod-shaped cluster nucleation pathway for glucose isomerase is perhaps more reminiscent of the cluster-cluster interaction at high supersaturation that is described by classical nucleation theory".

[1] D. Gebauer, A. Völkel, H. Cölfen, Stable Prenucleation Calcium Carbonate Clusters, *Science* **2008**, *322*, 1819−1822.
[2] N. D. Loh, S. Sen, M. Bosman, S. F. Tan, J. Zhong, C. A. Nijhuis, P. Král, P. Matsudaira, U. Mirsaidov, Multistep Nucleation of Nanocrystals in Aqueous Solution, *Nat. Chem.* **2017**, *9*, 77−82.
[3] B. Jin, Y. Wang, Z. Liu, A. France-Lanord, J. C. Grossman, C. Jin, R. Tang, Revealing the Cluster-Cloud and Its Role in Nanocrystallization, *Adv. Mater.* **2019**, *31*, 1808225.
[4] M. Sleutel, A. E. Van Driessche, Role of Clusters in Nonclassical Nucleation and Growth of Protein Crystals, *Proc. Natl. Acad. Sci. USA* **2014**, *111*, E546–E533.
[5] E. Wiedenbeck, M. Kovermann, D. Gebauer, H. Cölfen, Liquid Metastable Precursors of Ibuprofen as Aqueous Nucleation Intermediates, *Angew. Chem. Int. Ed.* **2019**, *58*, 19103−19109.
[6] Y. Tsarfati, I. Biran, E. Wiedenbeck, L. Houben, H. Cölfen, B. Rybtchinski, Continuum Crystallization Model Derived from Pharmaceutical Crystallization Mechanisms. *ACS Cent. Sci.* **2021**, *7*, 900–908.